Mausam, (1990), **41**, 2, 265-268

551.509.33 : 551.553.21

A regional model for monsoon prediction

[S. S. SINGH, S. S. VAIDYA and E. N. RAJAGOPAL

Indian Institute of Tropical Meteorology, Pune

सार – मानसून प्रगुक्ति के लिए निदर्श के पूर्वानुमान क्षमता का मूल्यांकन करने के लिए 13 सिनॉप्टिक विश्लेषणों के निवेश का प्रयोग करते हुए 48 घटों तक एक क्षेत्रीय छः स्तरीय पूर्वग समीकरण निदर्श का समाकलन किया गया है। निवेश विश्लेषणों में प्रभावी सिनॉप्टिक लक्षण मानसून अवदाब हैं। प्रागुक्ति गति और चक्रवातीय परिचालनों की प्रावस्था गति, निम्नस्तरीय जेट की शक्ति और स्थिति संकरण-भूमध्यरेखीय प्रवाह का अनुकरण और वर्षा का परीक्षण किया गया है।

ABSTRACT. A regional six-level primitive equation model has been integrated up to 48 hrs using input of 13 synoptic analyses to evaluate the forecast potential of the model for monsoon prediction. The dominant synoptic features in the input analyses are the monsoon depressions. The predicted movement and phase speed of cyclonic circulations, the low level jet's strength and position, the simulation of cross-equatorial flow and rainfall rates are examined.

1. Introduction

A regional six-level primitive equation model in sigma coordinate was developed for monsoon prediction (Singh *et al.* 1990) and tested with three synoptic days as input. The forecast results were found encouraging. In order to evaluate the forecast potential of the model for monsoon prediction, extensive testing of the model using data of June, July and August 1979 was taken up. We have integrated the model with input of 13 synoptic days. The paper presents the forecast verification statistics based on the results obtained so far.

2. Description of the model

The model equations are in sigma coordinate on Mercator projection and in flux form. The σ is defined as

$$\sigma = \frac{p - p_T}{p_s - p_T} \tag{1}$$

p_s is the surface pressure and p_T is the top of the model atmosphere which is 100 mb in the present model. The $p_s - p_T$ is denoted as π. The pressure p at any point on σ level is related with π as follows :

$$p = \sigma \pi + p_T \tag{2}$$

The set of equations are as follows :

(*i*) *Momentum equations*

$$\frac{\partial}{\partial t}\left(\frac{\pi}{m^2} u\right) = -\frac{\partial}{\partial x}(u^* u) - \frac{\partial}{\partial y}(v^* u) - \frac{\partial}{\partial \sigma}\left(\frac{\pi}{m^2}\dot{\sigma} u\right) + \frac{\pi}{m^2} v\left\{f - v\frac{\partial m}{\partial x} + u\frac{\partial m}{\partial y}\right\} - \frac{\pi}{m}\frac{\partial \phi}{\partial x} - c_p \frac{\pi\theta}{m}\frac{\partial P^\kappa}{\partial x} + \frac{\pi}{m^2} F_u + \frac{g}{m^2}\left(\frac{\partial \vec{\tau}}{\partial \sigma}\right)_x \tag{3}$$

$$\frac{\partial}{\partial t}\left(\frac{\pi}{m^2} v\right) = -\frac{\partial}{\partial x}(u^* v) - \frac{\partial}{\partial y}(v^* v) - \frac{\partial}{\partial \sigma}\left(\frac{\pi}{m^2}\dot{\sigma} v\right) - \frac{\pi}{m^2} u\left\{f - v\frac{\partial m}{\partial x} + u\frac{\partial m}{\partial y}\right\} - \frac{\pi}{m}\frac{\partial \phi}{\partial y} - c_p \frac{\pi\theta}{m}\frac{\partial P^\kappa}{\partial y} + \frac{\pi}{m^2} F_v + \frac{g}{m^2}\left(\frac{\partial \vec{\tau}}{\partial \sigma}\right)_y \tag{4}$$

(*ii*) *Thermodynamic energy equation*

$$\frac{\partial}{\partial t}\left(\frac{\pi}{m^2}\theta\right) = -\frac{\partial}{\partial x}(u^*\theta) - \frac{\partial}{\partial y}(v^*\theta) - \frac{\partial}{\partial \sigma}\left(\frac{\pi}{m^2}\dot{\sigma}\theta\right) + \frac{\pi}{m^2} F_\theta + \frac{\pi}{m^2} Q + \frac{g}{c_p}\frac{1}{m^2 P^\kappa}\frac{\partial H}{\partial \sigma} \tag{5}$$

(*iii*) *Equation for water vapour*

$$\frac{\partial}{\partial t}\left(\frac{\pi}{m^2} q\right) = -\frac{\partial}{\partial x}(u^* q) - \frac{\partial}{\partial y}(v^* q) - \frac{\partial}{\partial \sigma}\left(\frac{\pi}{m^2}\dot{\sigma} q\right) + \frac{\pi}{m^2} F_q + \frac{\pi}{m^2} M + \frac{g}{m^2}\frac{\partial E}{\partial \sigma} \tag{6}$$

(*iv*) *Continuity tendency and* $\dot{\sigma}$ *equations*

$$\frac{\partial}{\partial t}\left(\frac{\pi}{m^2}\right) = -\frac{\partial u^*}{\partial x} - \frac{\partial v^*}{\partial y} - \frac{\partial}{\partial \sigma}\left(\frac{\pi\dot{\sigma}}{m^2}\right) \tag{7}$$

$$\frac{\partial}{\partial t}\left(\frac{\pi}{m^2}\right) = -\int_0^1 \left\{\frac{\partial u^*}{\partial x} + \frac{\partial v^*}{\partial y}\right\} d\sigma \tag{8}$$

$$\left(\frac{\pi\dot{\sigma}}{m^2}\right)_\sigma = \left(\frac{\pi\dot{\sigma}}{m^2}\right)_{\sigma+\Delta\sigma} + \int_\sigma^{\sigma+\Delta\sigma} \left\{\frac{\partial}{\partial t}\left(\frac{\pi}{m^2}\right) + \frac{\partial u^*}{\partial x} + \frac{\partial v^*}{\partial y}\right\} d\sigma \tag{9}$$

(*v*) *Hydrostatic equation*

$$\frac{\partial \phi}{\partial \sigma} = -c_p\,\theta\,\frac{\partial P^\kappa}{\partial \sigma} \tag{10}$$

(*vi*) *Gas law equation*

$$\alpha = \frac{RT}{\pi\sigma + p_T} \tag{11}$$

where,

$$u^* = u\,\frac{\pi}{m}$$

$$v^* = v\,\frac{\pi}{m}$$

$$\kappa = \frac{R}{c_p}$$

and

$$P = \left(\frac{p}{1000}\right)$$

$\vec{\tau}$ is the eddy stress of momentum F_u, F_v, F_θ and F_q are horizontal diffusion for u, v, θ and q respectively. H and E are vertical eddy flux of heat and water vapour respectively. Q is diabatic heating (cooling) per unit mass. M is change of water vapour per unit mass. Other symbols have their usual meanings.

A detailed description of the model is given by Singh *et al.* (1990). In vertical the model has six sigma levels. The model is staggered in the vertical with the horizontal wind components, geopotential height, temperature and mixing ratio for water vapour defined at the six sigma levels and the vertical σ velocity ($\dot{\sigma}$) defined at intermediate levels. The horizontal domain extends from 10° S to 40° N and 40° E to 115° E. The horizontal grid interval used is 150 km on Mercator projection. Arkawa's B-type of staggering is used in the horizontal. In horizontal, the time invariant boundary conditions areused. In vertical, the condition $\dot{\sigma} = 0$ at $\sigma=1$ and at $\sigma=0$ are used. Mass, energy, potential temperature and variance of potential temperature conserving finite difference scheme (Arakawa and Mintz 1974, Arakawa and Lamb 1977) for space derivatives is used in the model. The horizontal advection terms in the momentum equations are computed with fourth order accuracy finite difference scheme. Other terms are computed with second order accuracy scheme. For time integration the leap-frog scheme with Asselin (1972) time filter is used with a time step of 3 minutes. The physical processes included in the model are the large scale condensation, the dry convective adjustment, the Kuo type cumulus convection following Krishnamurti *et al.* (1976), the horizontal and vertical diffusion, the surface friction, the sensible heat supply and evaporation over the sea. Smoothed orography is included in the model. No initialization is carried out to the initial data. The objectively analysed data is used as input to the model.

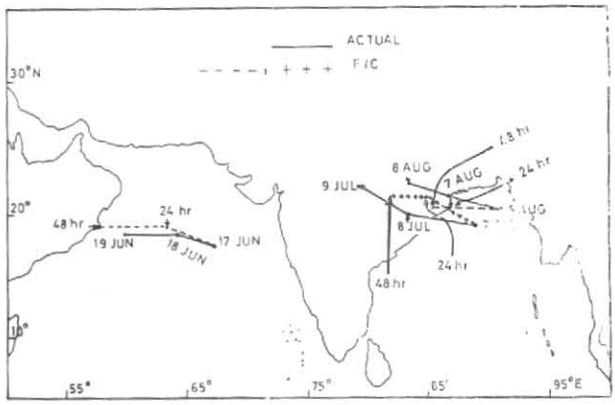

Fig. 1. Track of monsoon depressions at 850 mb for 17 June 1979, 7 July 1979 and 6 August 1979 input cases

3. Data

Three monsoon depression cases are selected for evaluating the forecast potential of the model. The data of 13 synoptic days has been used as input to the model, *viz.*, 15-17 June, 4-8 July and 5-9 August 1979. The monsoon depression was in the Arabian Sea in June and in the Bay of Bengal in July and August. The domain of integration was under the influence of depression for 6 to 7 days during each case.

The humidity data in the FGGE IIIb analysis in the vicinity of depression are found underestimated. We, therefore, manually analysed the moisture data for the depression area for 850, 700 and 500 mb levels. This analysed data was compared with the FGGE IIIb data. It was found that the analysed data was better than the FGGE IIIb data. As such, the manually analysed moisture data were used as input to the model at these three levels.

4. Forecast results

The model was integrated up to 48 hr using input data of 13 synoptic days, *viz.*, 15-17 June, 4-8 July and 5-9 August 1979. In all the cases 850 mb level winds are examined to evaluate the forecast potential of the model. Synoptic features examined are : movement of the depression, phase speed, low level jet's strength and position and the simulation of cross-equatorial flow. The rainfall rates are also examined. The predicted rainfall rates are compared with the observed rainfall rates given by Krishnamurti *et al.* (1983).

(a) *Wind*

In all cases, the model is able to simulate the cross-equatorial flow, low level jet over Arabian Sea and circulations along the equator. In general, the predicted easterlies to the north and westerlies to the south of

TABLE 1

Observed *versus* predicted phase speed and position vector error based on 13 synoptic days of monsoon depression

Input 12 GMT	Phase speed (km/24 hr)				Vector error (km)	
	0-24 hr		24-48 hr		24-hr	48-hr
	F/C	Obs.	F/C	Obs.	F/C	F/C
15 Jun	360	90	860	560	440	90
16 Jun	330	560	720	330	490	220
17 Jun	430	330	640	480	110	250
Aver.	373	327	740	457	347	187
4 Jul		270	245	200		220
5 Jul	250	180	400	200	100	300
6 Jul	180	200	290	610	90	320
7 Jul	520	610	240	490	230	350
8 Jul	260	490		260	340	
Aver.	303	350	294	352	190	323
5 Aug			230	450		210
6 Aug	420	450	190	380	110	280
7 Aug	530	380		490	200	
8 Aug	170	490		370	320	
9 Aug	110	370	650	490	330	150
Aver.	308	423	420	436	240	213
Aver. of 13 days	328	367	484	415	259	241

F/C—Forecast, Obs.—Observed

TABLE 2

RMS error for u and v (ms^{-1}) at 850 and 200 mb

Input 12 GMT (Date)	850 mb				200 mb			
	24-hr		48-hr		24-hr		48-hr	
	u	v	u	v	u	v	u	v
				June				
15	4.40	3.65	4.94	4.20	5.89	4.89	7.23	6.93
16	4.83	4.51	5.95	6.27	6.55	5.34	6.86	5.60
17	3.80	3.62	4.77	4.03	5.82	4.70	7.21	4.73
Aver.	4.34	3.93	5.22	4.83	6.09	4.98	7.10	5.75
				July				
4	3.62	3.22	3.94	3.97	4.79	5.22	6.90	6.50
5	3.14	3.60	3.90	3.92	5.41	5.32	6.71	7.35
6	3.11	3.56	4.56	4.24	4.90	4.96	6.84	5.78
7	3.44	3.39	4.53	3.59	4.77	4.71	6.75	4.60
8	3.50	3.70	5.78	4.23	4.48	4.02	7.52	5.80
Aver.	3.36	3.49	4.54	3.99	4.87	4.84	6.92	6.01
				August				
5	4.85	3.74	5.84	4.30	7.17	7.24	9.41	8.43
6	4.18	3.63	4.65	4.04	6.48	6.32	6.46	4.84
7	4.34	3.76	4.65	4.80	6.04	4.55	7.73	5.25
8	4.19	4.19	4.40	4.50	6.30	5.23	9.06	6.22
9	3.51	3.54	4.03	3.98	6.38	5.71	8.99	5.44
Aver.	4.21	3.77	4.71	4.32	6.47	5.81	7.93	6.03

the centre of depression are found to be weaker than the observed whereas, the strength of the low level jet is overpredicted.

The input showed a deep depression over Arabian Sea centred at 17.6° N, 67.1° E, the low level jet over Arabian Sea with the core along 10° N and strength of 50 kt, the crossequatorial flow along 40°-60° E and a cyclonic circulation near the equator at 65° E. The forecast wind charts showed that the cyclonic circulation associated with the depression was simulated well. The forecast centre of the depression was at 63.5° E, 19° N in the 24-hr forecast and in the 48-hr forecast the centre was at 57° E, 19° N. The verification charts showed the depression centre at 64.1° E, 18.4° N on18 June and at 59.8° E, 18.4° N on 19 June 1979. Hence in this case the predicted movement of the depression was faster than the observed movement. The easterlies to the north of the depression were underpredicted. The cross-equatorial flow was predicted well. The circulations near the equator were also predicted well. A narrow band of strong westerlies of 60 kt speed was seen over the Arabian Sea along 10°-12° N in the forecast charts, whereas in the verification charts a broad band of westerlies of speed 40 kt was seen.

Fig. 1 shows the track of the depression for 17 June, 7 July and 6 August 1979 input cases. It is seen that in 17 June case the forecast movement of the depression is faster than the observed, although the direction of movement is correctly predicted. In 7 July and 6 August cases the predicted movement is slower than the observed.

In Table 1 we present observed phase speeds, predicted phase speeds and the position vector errors for the 13 days of input. In general, the predicted phase speed is more than the observed and the position vector error is less in the 48-hr forecast as compared to 24-hr in June cases. In July and August cases, in general, the predicted movement is slower than the observed and the position vector error is more in the 48-hr forecast.

Table 2 shows the R.M.S. error for u and v components at 850 mb and 200 mb levels. From Table 2 it is seen that R.M.S. error is more in the 48-hr forecast for both u and v components.

(b) *Rainfall*

In general, the rainy area is predicted well in all the cases. Table 3 shows threat score, predicted and observed mean rainfall for 10^5 km^2 area around the depression and predicted and observed maximum rainfall amount associated with depression for June and July cases.

Threat score T_s is defined by :

$$T_s = \frac{C}{F + R - C}$$

TABLE 3

Threat score, predicted and observed mean rainfall for 10^5 km^2 area around the depression and predicted and observed maximum rainfall value associated with depression

Input (Date)	Threat score	Mean rainfall for the area (10^5 km^2) around the depression (mm/24 hr)		Max. rainfall associated with depression (mm/24 hr)	
		Pred.	Obs.	Pred.	Obs.
		June			
15	0.48	26	30	51	35
16	0.12	15	30	28	35
17	0.54	25	30	54	35
		Ju			
4	0.07	22	130	99	141
5	0 18	42	40	102	55
6	0.24	10	29	39	21
7	0.24	12	50	40	55
8	0.14	5	50	17	59

Pred.—Predicted, Obs. — Observed

where, C is the number of grid points correctly forecast to receive a threshold amount of rainfall (=0.2 mm day), F is the number of grid points forecasting the threshold amount and R is the number of grid points observing the threshold amount.

From the above relation for threat score it can be seen that T_s can vary from 0 to 1. When T_s=1 the predicted and observed areal distribution of rainfall match each other. The threat score gives a quantitative information about the areal distribution of predicted rainfall.

From Table 3 the threat score values indicate that the areal distribution of rainfall is predicted better in 15 June and 17 June input cases as compared to other days. The predicted mean rainfall for 10^5 km^2 area around the depression is found to be comparable with the observed in all cases except the 4 and 8 July cases. Table 3 also shows that the predicted maximum rainfall amount associated with the system are underpredicted in 4 cases and overpredicted in other cases.

5. Concluding remarks

A regional six-level primitive equation model in sigma coordinate has been integrated with input of 13 synoptic days for evaluation the forecast potential of the model for monsoon prediction. The results discussed are summarised as follows :

(*i*) In all 13 cases, in general, the prediction is satisfactory up to 48 hr.

(*ii*) The flow pattern, cross-equatorial flow and the structure of the monsoon depression are predicted well.

(*iii*) The direction of movement of the depression is predicted well. The speed of movement is overpredicted in some cases while it is underpredicted in other cases.

(*iv*) The R.M.S. errors for both u and v components are more in the 48-hr than in 24-hr forecast fields.

(*v*) The areal distribution of rainfall is predicted well. The rainfall rates are overpredicted in some cases while it is underpredicted in other cases.

The results reported here are based on the results obtained from 13 cases. The model will be extensively tested and the model forecast potential will be investigated.

Acknowledgements

The authors would like to thank the Director, Indian Institute of Tropical Meteorology, Pune for his keen interest in the study.

References

Arakawa, A. and Lamb, V.R., 1977, Computational design of the basic dynamical processes of the UCLA general circulation model, *Methods in computational Physics*, **17**, 173-265.

Arakawa, A. and Mintz, Y., 1974, The UCLA Atmospheric General Circulation Model (with the partcipation of A. Katayama, J.W. Kim, W. Schubert, T. Topkioka, M. Schlesinger, W.Chao, D. Randall and L. Lord) Notes distributed at the Workshop, 25 March-4 April 1974, Dep. of Met., Univ. of California.

Asselin, R., 1972, Frequency filter for time integration, *Mon. Weath. Rev.*, **100**, 487-490.

Krishnamurti, T.N., Kananitsu, M., Godbole, R., Chang, C.B., Carr, F. and Chow, J., 1976, A study of a monsoon depression: II-Dynamical structure, *J. met. Soc. Japan*, **54**, 208-225.

Krishnamurti, T.N., Steven Cocke, Richard Pasch & Simon low-Nam, 1983, Precipitation estimates from raingauge and satellite observations summer MONEX.

Singh, S.S., Vaidya, S.S. and Rajagopal, E.N., 1990, A limited area model for monsoon prediction, *Adv. in Atmos. Sci.*, **7**, 1, 111-126.